ELSEVIER

Ceramics International 25 (1999) 671–676

CERAMICS INTERNATIONAL

Effect of minor binder on capillary structure evolution during wicking

Sang Woo Kim*, Hae-Weon Lee, Huesup Song

Ceramic Processing Center, Korea Institute of Science and Technology, PO Box 131, Cheongryang, Seoul, Korea

Received 10 May 1998; received in revised form 10 July 1998; accepted 3 August 1998

Abstract

The wax-based binder system showed discrete transition behavior in capillary structure during debinding due to the rapid redistribution of major binder, e.g. paraffin wax. Depending on the minor binder added, the transition behavior in capillary structure was significantly altered presumably due to the difference in chemical compatibility between major and minor binders. Limited chemical compatibility between major and minor binders might promote the funicular to pendular transition because of the segregation of polar minor binder in the nonpolar paraffin wax matrix. It was also demonstrated that the thermal pyrolysis should be initiated with increased temperature just past the funicular to pendular transition point in order to reduce the total debinding time.

Keywords: Wax-based binder; Capillary structure; Wicking

1. Introduction

Binder removal is a key step for successful ceramic injection molding [1,2]. The binder must be removed from the molded part prior to its densification by sintering. Binder systems can consist of several organic ingredients, each with a markedly different melt viscosity as well as with different decomposition characteristics. These ingredients must be removed slowly, in a process that requires the gradual formation of passages within the part with increasing temperature and time. These passage allow the major binder ingredient to escape at higher temperatures without causing the part to deform or crack [3–6].

Although there are many debinding methods available [7,8], wicking process that extracts the binder through capillary action has several advantages [9–12]. It provides additional support, better thermal uniformity, reduction in gas partial pressure gradients at the surface of the part, and homogeneous wicking out of the binder throughout the part [13–15]. In particular, the low-pressure injection-molded parts with low melting point and low viscosity binder are vulnerable to deformation and slumping during debinding process [16–18]. The wicking process is the choice of methods for the parts of complicated shapes fabricated by low pressure injection molding.

The debinding process of green bodies is the process in which the volume occupied by the binder system is gradually becoming the pore [19,20]. Therefore, the debinding process may be well described by the variation of the degree of saturation [21] which is defined by the ratio of the volume occupied by the binder system to the available pore volume. Since the mixtures for injection molding usually contain ceramic powders of less than the critical volume fraction to achieve an appropriate viscosity for forming, green bodies are in the fluid state at the very beginning of debinding. In addition, the thermal expansion of the liquid binder induces hydraulic pressure in the capillaries, which enhances binder removal rate [20]. As the excess amount of the binder system is removed, the green bodies reach the capillary state in which the volume of the binder system equals available pore volume. After the capillary state has been achieved, actual pores develop in the green bodies, but the binder system maintains a continuous phase, which is the funicular state. With further progress of debinding the binder system becomes isolated around the particles and pores form a continuous phase, which corresponds to the pendular state [21–23].

* Corresponding author. Tel.: +82-2-958-5526; fax: +82-2-958-5529.
E-mail address: swkim@kistmail.kist.re.kr (J.W. Kim)

0272-8842/99/$ - see front matter
PII: S0272-8842(98)00082-0

The authors [24] have already demonstrated from pore structure evolution during wicking that there occur several transitions in capillary structure due to the rapid redistribution of binder. In that study, the polyethylene wax was used as minor binder with paraffin wax as major binder. At the wicking temperature, polyethylene wax has almost two orders of magnitude higher melt viscosity than paraffin wax. Paraffin wax can be easily removed through pore channel by capillary attraction because melt viscosty of Paraffin wax is sufficiently low. Since polyethylene wax is a kind of saturated hydrocarbon, it is more compatible with paraffin wax than minor binder with high polarity such as ethylene–vinyl acetate copolymer. The difference of chemical affinity between two polymers may affect the microstructural properties of mixtures of binder and powder.

The objective of the present study is to investigate the effect of the type of minor binder on the removal process of major binder and the pore structure evolution of partially debinded body in the course of the wicking of compression-molded parts.

2. Experimental methods

2.1. Materials and preparation of green bodies

The ceramic powder used in this study was a commercial silicon nitride and the binder system consisted of paraffin wax, ethylene–vinyl acetate copolymer (EVA), polyethylene wax (PE wax), and stearic acid. The role and properties of each component as well as the composition of the mixture are summarized in Table 1.

The silicon nitride powder and the binder system were mixed as follows. The silicon nitride powder was first coated with the stearic acid by adding the powder in the ethanol solution of stearic acid at 50°C, then the ethanol was removed by evaporation. The coated silicon nitride powder was then mixed sequentially with minor binders such as ethylene–vinyl acetate copolymer and polyethylene wax at 100°C and with paraffin wax at 70°C.

The samples for measuring the debinding kinetics were formed by compression molding the mixture at 40°C under the pressure of 150 MPa. The compression molded samples were rectangular bars with a dimension of 35×8×3.5 mm.

2.2. Wicking debinding

For the wicking debinding, the bar samples, embedded in fine alumina powder, were put at the center of the 200 cm^3 alumina crucible. The alumina powder (AKP 30, Sumitomo, Japan) used as the powder bed had an average particle size of 0.35 μm. The whole assembly was tapped until the fractional density of the powder bed reached 28%, and was put in an electrical furnace at 150°C. The variation of sample weight with debinding time was measured.

2.3. Characterization

The pore size distributions of both the partially and completely debinded samples were measured with a mercury porosimeter (Poresizer 9320, Micromeritics, USA). To prepare the completely debinded sample the wicked body was further debinded by the thermal pyrolysis at 600°C. Resulting pore size distributions were presented on the volume basis, $D_V(r)$, which could be defined by the following equation:

$$D_V(r) = P/r(dV/dP)$$

Here, r is the pore size, and V is the volume intruded by mercury at pressure P.

The strength of compression-molded bodies was measured by three point bending test by using Universal Testing Machine (Instron Co., 1127, USA). The test condition was cross speed, 5 mm/min and span length, 25 mm.

In order to examine the interaction between silicon nitride powder and minor binder, EVA, the adsorption isotherm by solution depletion method was carried out. The clear supernatant was obtained by centrifuging at 12,000 rpm for 30 min.

3. Results

Fig. 1 shows weight loss by wicking as a function of debinding time for the compression-molded parts

Table 1
Raw materials and its properties and compositions

Role	Raw material	Supplier	Grade	Particle size (μm)	Compositions of compression-molded bodies (wt%)			
Ceramic powder	Si_3N_4	Ube	SN E-10	0.5				
Binder system	Raw material	Supplier	Grade	Melting point (°C)	Powder	Major binder	Minor binder	Surfactant
Major binder	Paraffin wax	Dongnam	DP-135	57∼60	77.9	15.6	2.5	3.8
Minor binder	PE wax[a]	Lion Chemical	102N	108	77.8	14.1	4.1	3.9
Minor binder	EVA[a]	Elf Atochem	28-25	75	77.7	12.5	5.7	3.9
Surfactant	SA[a]	Stearic Acid	17-536-6	67–69				

[a] PE wax, polyethylene wax; EVA, ethylene–vinyl acetate copolymer; SA, stearic acid.

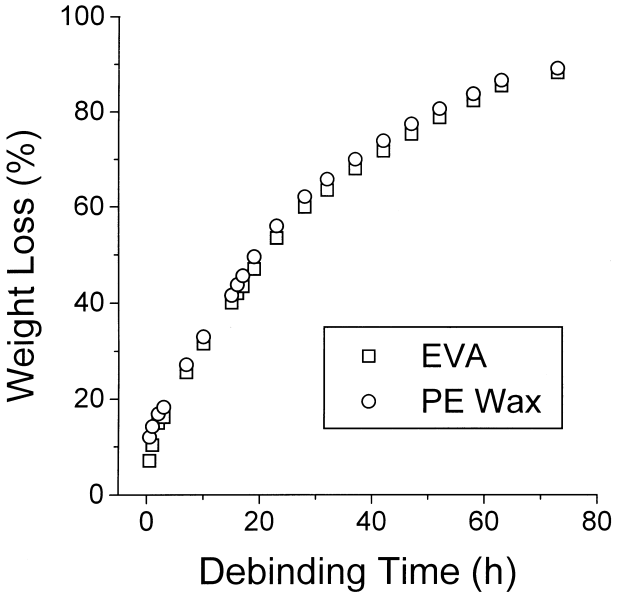

Fig. 1. Percent weight loss of major binder as a function of wicking time for the compression-molded parts containing: □, EVA; and ○, PE wax as a minor binder, respectively.

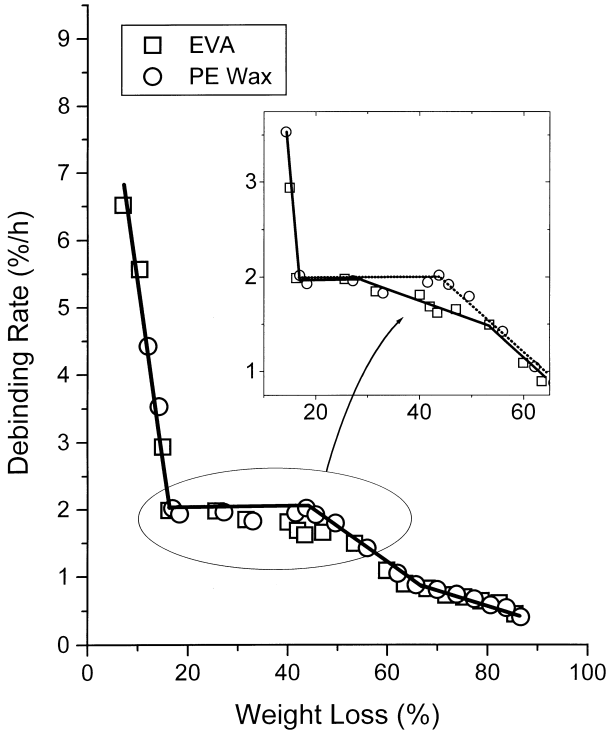

Fig. 2. Debinding rate as a function of %wt loss of major binder for the compression-molded parts containing: □, EVA; and ○, PE wax.

containing EVA and PE wax as minor binders, respectively. The percentage of weight loss was determined with respect to the amount of major binder, e.g. paraffin wax. In doing so, the solubility of PE wax and EVA in paraffin wax was neglected, since the mutual solubility, if any, does not appear to have a significant effect on debinding characteristics such as pore structure evolution and binder distribution, etc. There is essentially no difference in the debinding behavior for those parts containing EVA and PE wax as minor binders.

As previously described by the authors [24], the wicking rate depends on the capillary structure that is determined by pore structure as well as binder distribution. In order to evaluate the effect of the minor binder on the debinding behavior in detail, it might be instructive to examine the wicking rate dependency on the structural change of capillaries. Fig. 2 compares the debinding rate as a function of percent weight loss of major binder for the compression-molded parts containing EVA and PE wax. As expected, the variation of debinding rate with the decrease of remaining major binder can be generally divided into four regimes which correspond to various structural change in capillaries. It has been demonstrated in the previous study that debinding proceeds uniformly throughout green bodies with the help of the rapid redistribution of the binder system, especially paraffin wax [24]. In consequence, it is believed that the capillaries in the green bodies go through the structural changes as a whole. In all four regimes, both parts containing EVA and PE wax as minor binder shows very similar trend in the structural transitions of capillaries except the slight discrepancy found in the second and third regimes.

In order to compare the discrepancy in the second and third regimes, Fig. 2 is magnified in the weight loss of 10–65%. Now, it is quite evident that there is a considerable difference in debinding behavior for those parts with EVA and PE wax in that there exists another transition point in the parts with EVA. It has been suggested that the point C is related to the structural change of capillaries from funicular to pendular state. Contrary to the parts containing PE wax, those with EVA shows an additional transition in debinding rate versus percent weight loss relation corresponding to point B. It is likely that the type of minor binder has a significant effect on the structural change in capillaries during wicking.

In order to correlate the observed discrepancy in debinding behavior between EVA and PE wax containing parts, the pore size distributions of partially debinded bodies were compared as shown in Fig. 3. It is evident that the pore size distributions also show quite a difference between EVA and PE wax containing bodies in that the bodies with EVA can reach close to that of almost fully wicked bodies after removing about 52% of major binder. The difference in pore structure evolution in both green bodies after partial debinding shows a good agreement with the structural changes in capillaries observed in Fig. 2. Thus far, although the debinding behavior of the compression-molded body was generally described in terms of the amount of remaining binder and/or debinding time, it might be

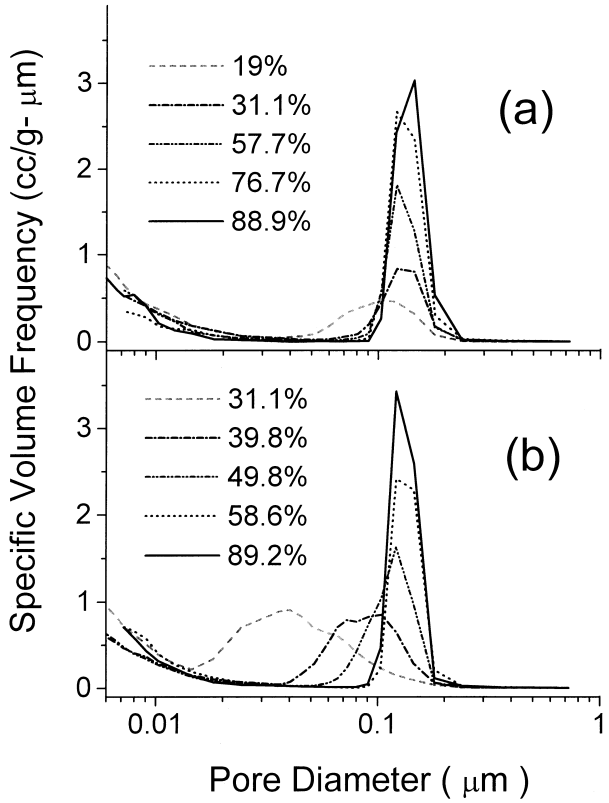

Fig. 3. Pore size distributions of partially debinded bodies for the compression-molded parts containing: (a) EVA and (b) PE wax.

necessary to take the binder composition and the mutual compatibility among components.

4. Discussion

In general, the debinding process of the injection-molded bodies with wax based binders consists of wicking of major binder and subsequent thermal pyrolysis of the residual component including minor binder. In order to reduce total debinding time, it is necessary to correctly determine the time to switch from wicking to thermal pyrolysis. As shown in Fig. 2, the variation of debinding rate as a function of the amount of major binder removed might provide an insight into the structural changes in capillaries which is crucial in determining the time for switching from wicking to thermal pyrolysis. The wicking process takes place by capillary flow of major binder as long as the major binder maintains a continuous channel. However, once the major binder starts to become discontinuous to form isolated pockets of major binder, the wicking process is no longer effective for binder removal. Therefore, it is necessary to activate thermal pyrolysis by raising temperature, which takes place by internal evaporation or thermal decomposition and subsequent gas diffusion toward surface. During thermal pyrolysis process, the gas species produced by internal evaporation and thermal decomposition should escape without pressure buildup inside the green bodies. Therefore, it is required to obtain a partially debinded bodies with continuous pore channels throughout green bodies in order to activate next debinding process by evaporation and/or thermal decomposition.

As mentioned previously [24], the major binder, e.g. paraffin wax, has very low viscosity at the wicking temperature so that it can readily redistribute itself due to the capillary pressure. In general, the right time to raise debinding temperature is just after entering the third regime in Fig. 2 where the capillary structure go through the transition from funicular to pendular state. In other words, it is likely that the capillary structure barely maintains funicular state at the end of the second regime, with most pore channels connected. Fig. 4 shows the fully debinded rectangular bars, which are debinded just before and after reaching transition point C in Fig. 2. The partially debinded parts were heated at the rate of 5°C/min up to 600°C and held at 600°C for 2 h for thermal decomposition of the residual binders. It is evident that the green bodies debinded past the point C in Fig. 2 shows good dimension tolerance without debinding defects such as distortion and/or cracks. Therefore, employing the thermal pyrolysis just past the constant debinding period can substantially reduce total debinding time without excessive wicking time.

Since the transition point of capillary structure from funicular to pendular state is a good indicator for switching debinding mechanism from wicking to thermal pyrolysis, the difference in wicking behavior between EVA and PE wax containing bodies could have a significant meaning in determining total debinding. Fig. 2 is replotted in a form of debinding rate versus debinding time in Fig. 5. It takes about 8.3 h for the bodies with EVA to reach the end point of the constant rate period by wicking, while it does about 16 hours for those with PE wax. Assuming that it takes 4 h for thermal pyrolysis after

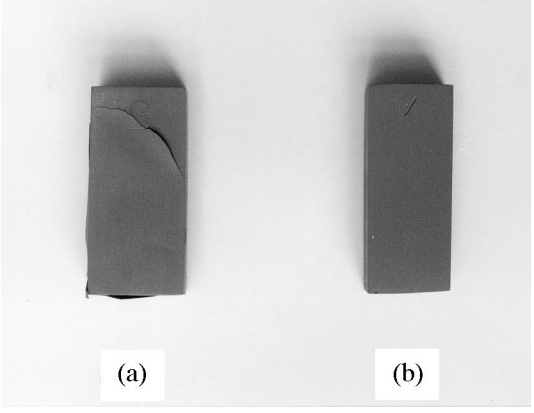

Fig. 4. Photographs of the fully debinded bodies which are wicked (a) just before and (b) just after reaching transition point C in Fig. 2

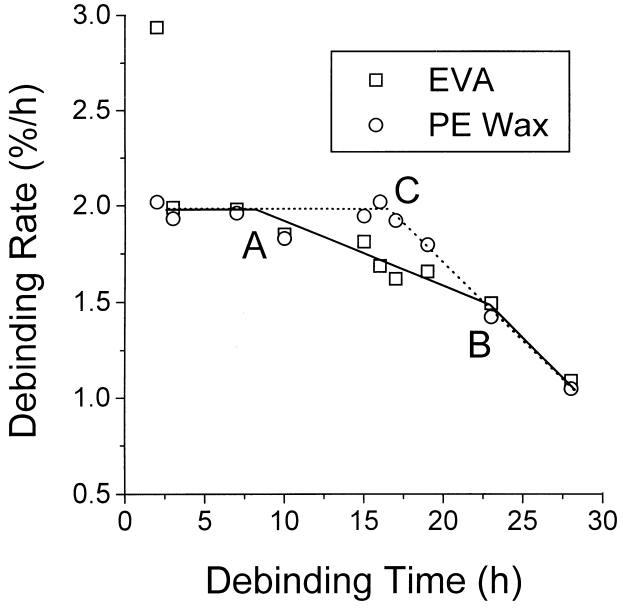

Fig. 5. Debinding rate as a function of wicking time for the compression-molded parts containing: □, EVA; and ○, PE wax.

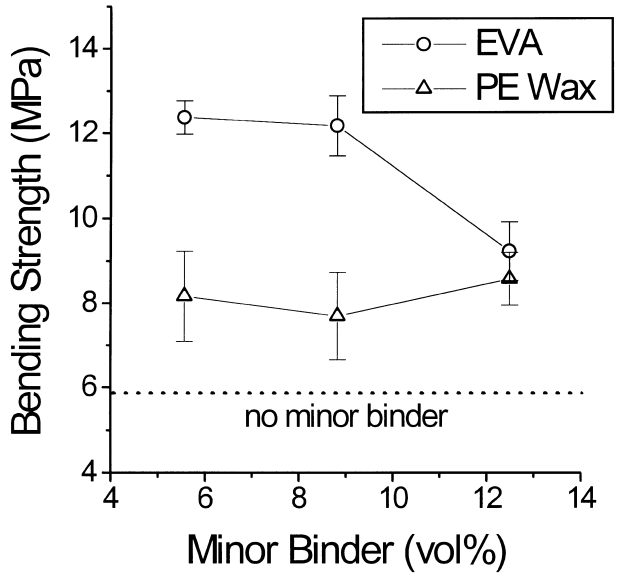

Fig. 6. Green strength of compression-molded bodies containing: □, EVA; and ○, PE wax as a function of the amount of minor binder added.

wicking, it is possible to reduce total debinding time by about 38% just by choosing EVA instead of PE wax as minor binder.

However, it could not be clearly explained why the parts with EVA goes though early transition from funicular to pendular state in capillary structure as shown in Fig. 2. Fig. 6 shows a plot of green strength of compression-molded body containing both EVA and PE wax as a function of the amount of minor binder added. When the minor binder was added, the green strength of compression-molded bodies increased by 50–200%,

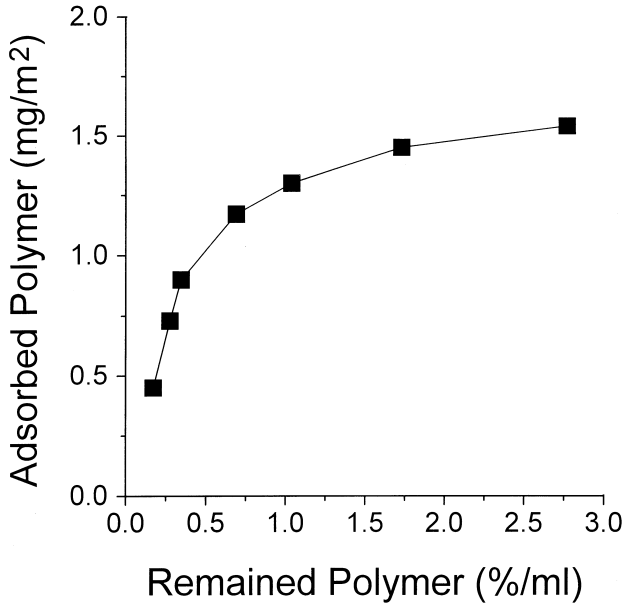

Fig. 7. Isothermal adsorption curve of the mixtures containing EVA.

depending on the type and amount of the minor binder. In particular, the green strength of compression-molded body with EVA was much higher than that with PE wax. The green strength of compression-molded bodies is dependent on various variables such as binder strength, adhesion strength between binder and particle surface, powder characteristic, powder volume fraction, mixture homogeneity, and so on. The increased strength with EVA addition might be attributed to the improved adhesion strength between the acetate group of EVA and hydroxyl group on particle surface. With respect to the difference in debinding behavior observed in the second and third regimes in Fig. 2, the reduced strength of green bodies with 12.5% EVA addition might be more instructive and informative. This significant decrease in green strength could be ascribed to EVA segregation due to the limited chemical compatibility between EVA and paraffin wax. This was confirmed by the adsorption isotherm determined by solution depletion method, as shown in Fig. 7. It can be found that the saturated amount of adsorbed EVA is about 1.5 mg/m^2 Si_3N_4 which corresponds to about 2.6 vol% of total volume of compression-molded body. Rest of EVA should be mechanically mixed with paraffin wax, which is the main reason for chemical incompatibility.

Therefore, it might be suggested that the chemical incompatibility is the principal reason for the deviation of debinding behavior of the compression-molded body containing EVA as minor binder. Even though it is not clear to which degree the chemical incompatibility can be allowed in the mixture formulation, it might be a useful tool for a rapid debinding to utilize the limited chemical incompatibility in binder formulation for injection molding.

5. Conclusions

The chemical compatibility between major and minor binders has a significant effect on the debinding behavior of the injection-molded body with wax based binders. In paraffin wax based binder system, the green bodies containing EVA as minor binder entered structural changes in capillaries from funicular to pendular state with the weight loss of about 30%, while those containing PE wax did with weight loss of about 50%. It is believed that the earlier completion of the constant debinding rate period might be beneficial for reducing total debinding time. Even in the pendular state, there was an extra transition point in the binder system composed of paraffin wax and EVA. This might be attributed to the limited chemical compatibility in the presence of excessive EVA as the amount of the major binder was preferentially removed by wicking.

References

[1] R.M. German, K.F. Hans, S.-T.P. Lin, Key issues in powder injection molding, Am. Ceram. Soc. Bull. 70 (1991) 1294–1302.
[2] M.J. Edirisinghe, Removal of the organic binder from moulded ceramic bodies, Proc. Br. Ceram. Soc. 54 (1990) 109–122.
[3] S.J. Stedman, J.R.G. Evans, J. Woodthorpe, A method for selecting organic materials for ceramic injection moulding, Ceramics International 16 (1990) 107–113.
[4] V.N. Shukla, D.C. Hill, Binder evolution from powder compacts, thermal profile for injection-molded articles, J. Am. Ceram. Soc. 72 (1989) 1797–1803.
[5] A. Johnson, E. Carlstrom, L. Hermansson, R. Carlsson, Rate-controlled extraction unit for removal of organic binders from injection moulded ceramics, in: P. Vincenzini (Ed.), Ceramic Powders, Elservier, Amsterdam, 1983, pp. 767–772.
[6] J.K. Wright, J.R.G. Evans, Removal of organic vehicle from moulded ceramic bodies by capillary action, Ceramics International 17 (1991) 79–87.
[7] R.M. German, Theory of thermal debinding, Int. J. Powder Met. 23 (1987) 237–245.
[8] R.M. German, The thermal debinding of injection molded powder compacts, Powder Met. Int. 22 (1990) 17–22.
[9] Y. Bao, J.R.G. Evans, Kinetics of capillary extraction of organic vehicle from ceramic bodies, part I: partitioning between porous media, J. Eur. Ceram. Soc. 8 (1991) 81–93.
[10] Y. Bao, J.R.G. Evans, Kinetics of capillary extraction of organic vehicle from ceramic bodies, part II: partitioning between porous media, J. Eur. Ceram. Soc. 8 (1991) 95–105.
[11] J.K. Wright, J.R.G. Evans, Removal of organic vehicle from moulded ceramic bodies by capillary action, Ceramics International 17 (1991) 79–87.
[12] M.J. Edirisinghe, Removal of the organic binder from moulded ceramic bodies, Proc. Br. Ceram. Soc. 54 (1990) 109–122.
[13] M.J. Cima, J.A. Lewis, A.D. Devoe, Binder distribution in ceramic greenware during thermolysis, J. Am. Ceram. Soc. 72 (1989) 1192–1199.
[14] T.M. Shaw, Liquid redistribution during liquid-phase sintering, J. Am. Ceram. Soc. 69 (1989) 27–34.
[15] M.J. Cima, M. Dudziak, J.A. Lewis, Observation of poly[vinyl butyral]–dibutyl phthalate binder capillary migration, J. Am. Ceram. Soc. 72 (1989) 1087–1090.
[16] C.A. Sundback, M.A. Costantini, W.H. Robbins, Part distribution during binder removal, in: V.J. Tennecy (Ed.), Ceramic Materials and Components for Engines, American Ceramic Society, Westerville, OH, 1989, pp. 191–200.
[17] V.N. Shukla, D.C. Hill, Binder evolution from powder compacts, thermal profile for injection-molded articles, J. Am. Ceram. Soc. 72 (1989) 1797–1803.
[18] A. Johnson, E. Carlstrom, L. Hermansson, R. Carlsson, Rate-controlled extraction unit for removal of organic binders from injection moulded ceramics, in: P. Vincenzini (Ed.), Ceramic Powders, Elservier, Amsterdam, 1983, pp. 767–772.
[19] H.M. Shaw, T.J. Hutton, M.J. Edirisinghe, On the formation of porosity during removal of organic vehicle from injection-moulded ceramic bodies, J. Mat. Sci. Lett. 11 (1992) 1075–1077.
[20] M.R. Barone, J.C. Ulicny, Liquid-phase transport during removal of organic binders in injection-molded ceramics, J. Am. Ceram. Soc. 73 (1990) 3323–3333.
[21] R.M. German, Particle Packing Characteristics, Metal Powder Industries Federation, Princeton, NJ, 1989.
[22] R.M. German, The thermal debinding of injection molded powder compacts, Powder Met. Int. 22 (1990) 17–22.
[23] G.W. Scherer, Theory of drying, J. Am. Ceram. Soc. 73 (1990) 3–14.
[24] S.W. Kim, H.-W. Lee, H. Song, B.H. Kim, Pore structure evolution during solvent extraction and wicking, Ceramics International 22 (1996) 7–14.